

## Adiabatic versus isocurvature non-Gaussianity

Article (Published Version)

Hikage, Chiaki, Munshi, Dipak, Heavens, Alan and Coles, Peter (2010) Adiabatic versus isocurvature non-Gaussianity. *Monthly Notices of the Royal Astronomical Society*, 404 (3). pp. 1505-1511. ISSN 0035-8711

This version is available from Sussex Research Online: <http://sro.sussex.ac.uk/id/eprint/44527/>

This document is made available in accordance with publisher policies and may differ from the published version or from the version of record. If you wish to cite this item you are advised to consult the publisher's version. Please see the URL above for details on accessing the published version.

### **Copyright and reuse:**

Sussex Research Online is a digital repository of the research output of the University.

Copyright and all moral rights to the version of the paper presented here belong to the individual author(s) and/or other copyright owners. To the extent reasonable and practicable, the material made available in SRO has been checked for eligibility before being made available.

Copies of full text items generally can be reproduced, displayed or performed and given to third parties in any format or medium for personal research or study, educational, or not-for-profit purposes without prior permission or charge, provided that the authors, title and full bibliographic details are credited, a hyperlink and/or URL is given for the original metadata page and the content is not changed in any way.

# Adiabatic versus isocurvature non-Gaussianity

Chiaki Hikage,<sup>1\*</sup> Dipak Munshi,<sup>2</sup> Alan Heavens<sup>2</sup> and Peter Coles<sup>3</sup>

<sup>1</sup>*Department of Astrophysical Sciences, Princeton University, Peyton Hall, Princeton, NJ 08544, USA*

<sup>2</sup>*Scottish Universities Physics Alliance (SUPA), Institute for Astronomy, University of Edinburgh, Blackford Hill, Edinburgh EH9 3HJ*

<sup>3</sup>*School of Physics and Astronomy, Cardiff University, Cardiff CF24 3AA*

Accepted 2010 January 14. Received 2009 November 26; in original form 2009 July 2

## ABSTRACT

We study the extent to which one can distinguish primordial non-Gaussianity (NG) arising from adiabatic and isocurvature perturbations. We make a joint analysis of different NG models based on various inflationary scenarios: *local-type* and *equilateral-type* NG from adiabatic perturbations and *local-type* and *quadratic-type* NG from isocurvature perturbations together with a foreground contamination by point sources. We separate the Fisher information of the bispectrum of cosmic microwave background temperature and polarization maps by  $l$  for the *skew spectrum* estimator introduced by Munshi and Heavens to study the scale dependence of the signal-to-noise ratio of different NG components and their correlations. We find that the adiabatic and the isocurvature modes are strongly correlated, though the phase difference of acoustic oscillations helps to distinguish them. The correlation between local- and equilateral-type is weak, but the two isocurvature modes are too strongly correlated to be discriminated. Point source contamination, to the extent to which it can be regarded as white noise, can be almost completely separated from the primordial components for  $l > 100$ . Including correlations among the different components, we find that the errors of the NG parameters increase by 20–30 per cent for the *Wilkinson Microwave Anisotropy Probe* 5-year observation, but  $\simeq 5$  per cent for *Planck* observations.

**Key words:** methods: analytical – methods: statistical – cosmic microwave background – early Universe.

## 1 INTRODUCTION

The statistical properties of fluctuations in the early Universe can be used to probe the very earliest stages of its history, and provide valuable information on the mechanisms which ultimately gave rise to the existence of structure within it. This may include evidence for the cosmic inflationary expansion. With the recent claim of a detection of non-Gaussianity (NG; Yadav & Wandelt 2008) in the *Wilkinson Microwave Anisotropy Probe* (WMAP) sky maps, interest in primordial NG has obtained a tremendous boost.

NG from the simplest inflationary models based on a single slowly rolling scalar field is typically very small (Salopek & Bond 1990; Falk et al. 1993; Gangui et al. 1994; Acquaviva et al. 2003; Maldacena 2003; Bartolo, Matarrese & Riotto 2006). Variants of the simple inflationary models can lead to much higher levels of NG, such as multiple fields (Linde & Mukhanov 1997; Lyth, Ungarelli & Wands 2003), modulated reheating scenarios (Dvali, Gruzinov & Zaldarriaga 2004), warm inflation (Gupta et al. 2002; Moss & Xiong 2007) and ekpyrotic model (Buchbinder, Khoury & Ovrut 2007; Creminelli & Senatore 2007; Koyama et al. 2007).

Different forms are proposed to describe primordial NG. Much interest has focused on *local-type*  $f_{\text{NL}}$  by which the NG of Bardeen's curvature perturbations is locally characterized (Gangui et al. 1994; Verde et al. 2000; Wang & Kamionkowski 2000; Komatsu & Spergel 2001; Babich & Zaldarriaga 2004):

$$\Phi(x) = \phi(x) + f_{\text{NL}}[\phi^2(x) - \langle \phi^2(x) \rangle], \quad (1)$$

where  $\phi$  is the linear Gaussian part of  $\Phi$ . This form is motivated by the single-field inflation scenarios and then many models predict NG in terms of  $f_{\text{NL}}$  (Bartolo et al. 2004a). Optimized estimators of the bispectrum, which is the leading correlation term in the local form, are introduced by Heavens (1998) and have been successively developed to the point where an estimator for  $f_{\text{NL}}$  saturates the Cramér–Rao bound for partial sky coverage and inhomogeneous noise (Komatsu, Spergel & Wandelt 2005; Cabella et al. 2006; Creminelli et al. 2006; Medeiros & Contaldi 2006; Smith & Zaldarriaga 2006; Creminelli, Senatore & Zaldarriaga 2007; Liguori et al. 2007; Komatsu et al. 2009; Smith, Senatore & Zaldarriaga 2009).

The local-type  $f_{\text{NL}}$  is sensitive to the bispectrum with squeezed-configuration triangles ( $k_1 \ll k_2 \simeq k_3$ ). Several models including the inflation scenario with non-canonical kinetic terms (Seery & Lidsey 2005; Chen, Easther & Lim 2007), Dirac–Born–Infeld models (Alishahiha, Silverstein & Tong 2004) and Ghost

\*E-mail: hikage@astro.princeton.edu

inflation (Arkani-Hamed et al. 2004) predict large NG signals in equilateral configuration triangles ( $\ell_1 \simeq \ell_2 \simeq \ell_3$ ), which is well described with *equilateral-type*  $f_{\text{NL}}$  (Babich, Creminelli & Zaldarriaga 2004).

NG arising from primordial isocurvature (entropy) perturbations has been discussed in the context of NG field potentials (Linde & Mukhanov 1997; Peebles 1999; Boubekur & Lyth 2006; Suyama & Takahashi 2008), the curvaton scenario (Lyth et al. 2003; Bartolo, Matarrese & Riotto 2004b; Beltran 2008; Moroi & Takahashi 2009), modulated reheating (Boubekur & Creminelli 2006), baryon asymmetry (Kawasaki, Nakayama & Takahashi 2009) and the axion (Kawasaki et al. 2008). Hikage et al. (2009) first put observational limits on the isocurvature NG using *WMAP* 5-year data.

In this paper, we make a joint analysis of the different NG models to estimate the extent to which one can decode each NG information from cosmic microwave background (CMB) temperature ( $T$ ) and  $E$  polarization ( $E$ ) maps obtained by *WMAP* and *Planck*. We separate Fisher information of the CMB bispectrum by different ranges of  $l$  to study at which angular scale each NG parameter has large signal-to-noise ratio (S/N) and correlations among different NG components weaken. This idea is based on a new estimator called *skew spectrum*, which Munshi & Heavens (2010) have introduced to measure a scale dependence of NG parameters, while the commonly used single skewness parameter (Komatsu et al. 2005) gives a single value averaged over all scales. The advantage of the new estimator is that it retains information on the source of the NG, which the commonly used one does not.

For our analysis, we adopt a set of cosmological parameters at the maximum likelihood values for a power-law  $\Lambda$  cold dark matter ( $\Lambda$ CDM) model from the *WMAP* 5-year data only fit (Dunkley et al. 2009):  $\Omega_b = 0.0432$ ,  $\Omega_{\text{CDM}} = 0.206$ ,  $\Omega_\Lambda = 0.7508$ ,  $H_0 = 72.4 \text{ km s}^{-1} \text{ Mpc}^{-1}$ ,  $\tau = 0.089$ ,  $n_\phi = 0.961$ . The amplitude of the primordial power spectrum is set to be  $2.41 \times 10^{-9}$  at  $k = 0.002 \text{ Mpc}^{-1}$ . The spectra of isocurvature perturbations are assumed to be scale-invariant. The radiation transfer functions for adiabatic and isocurvature perturbations are computed using the publicly available *CMBFAST* code (Seljak & Zaldarriaga 1996).

This paper is organized as follows. Different NG models from primordial adiabatic and isocurvature perturbations are introduced in Section 2. Section 3 presents a Fisher matrix analysis of these parameters in which we estimate the corresponding error expected from *WMAP* and *Planck* observations. Section 4 devotes to a summary.

## 2 MODELS OF PRIMORDIAL NON-GAUSSIANITY

We consider various forms to describe primordial NG from adiabatic and isocurvature perturbations, and then provide explicit expressions for the bispectra.

### 2.1 Local-type adiabatic component

The bispectrum in the *local-type* NG form (equation 1) is written as (e.g. Verde et al. 2000; Komatsu & Spergel 2001)

$$B^{\text{Adi.Loc}}(k_1, k_2, k_3) = 2f_{\text{NL}}^{\text{Adi.Loc}} [P_\phi(k_1)P_\phi(k_2) + P_\phi(k_2)P_\phi(k_3) + P_\phi(k_3)P_\phi(k_1)], \quad (2)$$

where we rewrite  $f_{\text{NL}}$  in equation (1) as  $f_{\text{NL}}^{\text{Adi.Loc}}$ . The CMB angular bispectra for  $T$ ,  $E$  and their cross-terms are given by

$$b_{XYZ, l_1 l_2 l_3}^{\text{Adi.Loc}} = 2f_{\text{NL}}^{\text{Adi.Loc}} \int r^2 dr \left[ \beta_{Xl_1}^{\text{Adi}}(r)\beta_{Yl_2}^{\text{Adi}}(r)\alpha_{Zl_3}^{\text{Adi}}(r) + \beta_{Xl_1}^{\text{Adi}}(r)\alpha_{Yl_2}^{\text{Adi}}(r)\beta_{Zl_3}^{\text{Adi}}(r) + \alpha_{Xl_1}^{\text{Adi}}(r)\beta_{Yl_2}^{\text{Adi}}(r)\beta_{Zl_3}^{\text{Adi}}(r) \right], \quad (3)$$

where  $X$ ,  $Y$  and  $Z$  denote  $T$  or  $E$ , and  $\alpha_{Xl}^{\text{Adi}}$  and  $\beta_{Xl}^{\text{Adi}}$  are defined with the adiabatic radiation transfer function  $g_{Xl}^{\text{Adi}}$  as

$$\alpha_{Xl}^{\text{Adi}}(r) \equiv \frac{2}{\pi} \int k^2 dk g_{Xl}^{\text{Adi}}(k) j_l(kr), \quad (4)$$

$$\beta_{Xl}^{\text{Adi}}(r) \equiv \frac{2}{\pi} \int k^2 dk P_\phi(k) g_{Xl}^{\text{Adi}}(k) j_l(kr). \quad (5)$$

### 2.2 Equilateral-type adiabatic component

The bispectrum in the *equilateral-type* NG form is characterized by the NG parameter  $f_{\text{NL}}^{\text{Adi.Eq}}$  (Babich et al. 2004) as follows:

$$B^{\text{Adi.Eq}}(k_1, k_2, k_3) = 6f_{\text{NL}}^{\text{Adi.Eq}} \left\{ -P_\phi(k_1)P_\phi(k_2) - P_\phi(k_2)P_\phi(k_3) - P_\phi(k_3)P_\phi(k_1) - 2[P_\phi(k_1)P_\phi(k_2)P_\phi(k_3)]^{2/3} + [P_\phi(k_1)P_\phi(k_2)^2P_\phi(k_3)^3]^{1/3} + (5 \text{ perm.}) \right\}. \quad (6)$$

The CMB angular bispectra in this form are given by

$$b_{XYZ, l_1 l_2 l_3}^{\text{Adi.Eq}} = 6f_{\text{NL}}^{\text{Adi.Eq}} \int r^2 dr \left\{ -\beta_{Xl_1}^{\text{Adi}}(r)\beta_{Yl_2}^{\text{Adi}}(r)\alpha_{Zl_3}^{\text{Adi}}(r) - \beta_{Xl_1}^{\text{Adi}}(r)\alpha_{Yl_2}^{\text{Adi}}(r)\beta_{Zl_3}^{\text{Adi}}(r) - \alpha_{Xl_1}^{\text{Adi}}(r)\beta_{Yl_2}^{\text{Adi}}(r)\beta_{Zl_3}^{\text{Adi}}(r) - 2\delta_{Xl_1}^{\text{Adi}}(r)\delta_{Yl_2}^{\text{Adi}}(r)\delta_{Zl_3}^{\text{Adi}}(r) + [\beta_{Xl_1}^{\text{Adi}}(r)\gamma_{Yl_2}^{\text{Adi}}(r)\delta_{Zl_3}^{\text{Adi}}(r) + (5 \text{ perm.})] \right\}, \quad (7)$$

where

$$\gamma_{Xl}^{\text{Adi}}(r) \equiv \frac{2}{\pi} \int k^2 dk P_\phi^{1/3}(k) g_{Xl}^{\text{Adi}}(k) j_l(kr), \quad (8)$$

$$\delta_{Xl}^{\text{Adi}}(r) \equiv \frac{2}{\pi} \int k^2 dk P_\phi^{2/3}(k) g_{Xl}^{\text{Adi}}(k) j_l(kr). \quad (9)$$

### 2.3 Isocurvature components

Here, we consider an isocurvature perturbation  $\mathcal{S}$  between axion-type CDM and radiation, which is uncorrelated with adiabatic perturbations, defined as

$$\mathcal{S} \equiv \frac{\delta\rho_{\text{CDM}}}{\rho_{\text{CDM}}} - \frac{3\delta\rho_\gamma}{4\rho_\gamma}, \quad (10)$$

where  $\rho_{\text{CDM}}$  is the CDM energy density and  $\rho_\gamma$  is the radiation energy density. The fractional isocurvature perturbation  $f_S$  is defined as

$$f_S \equiv \frac{P_S(k_0)}{P_\zeta(k_0) + P_S(k_0)}, \quad (11)$$

where  $P_\zeta$  and  $P_S$  represent the power spectra of  $\zeta$  and  $\mathcal{S}$  and  $k_0$  is set to be  $0.002 \text{ Mpc}^{-1}$ . At linear order,  $\Phi$  (equation 1) is related to  $\zeta$  by  $\Phi = (3/5)\zeta$ . The definition of  $f_S$  is same as the commonly used parameter  $\alpha$  (Bean, Dunkley & Pierpaoli 2006). The current observational limit on  $f_S$  is 0.067 (95 per cent confidence level) for the axion-type isocurvature perturbation (Komatsu et al. 2009).

### 2.3.1 Local-type isocurvature component

We consider two different forms for isocurvature NG. One is the same local form as the adiabatic one (equation 1):

$$\mathcal{S}(\text{Lin}) = \eta + f_{\text{NL}}^{\text{Iso,Loc}}(\eta^2 - \langle \eta^2 \rangle), \quad (12)$$

where  $\eta$  is the linear Gaussian part. The bispectrum is given by

$$B_{XYZ,l_1l_2l_3}^{\text{Iso,Loc}}(k_1, k_2, k_3) = 2f_{\text{NL}}^{\text{Iso,Loc}} [P_\eta(k_1)P_\eta(k_2) + P_\eta(k_2)P_\eta(k_3) + P_\eta(k_3)P_\eta(k_1)], \quad (13)$$

The amplitude of the bispectrum is proportional to  $f_{\text{NL}}^{\text{Iso,Loc}} f_{\mathcal{S}(\text{Lin})}^2$  where  $f_{\mathcal{S}(\text{Lin})}$  represents the fractional isocurvature perturbation in the local form:

$$f_{\mathcal{S}(\text{Lin})} = \frac{P_{\mathcal{S}(\text{Lin})}}{P_{\mathcal{S}}} f_{\mathcal{S}}. \quad (14)$$

We obtain the CMB bispectrum as

$$b_{XYZ,l_1l_2l_3}^{\text{Iso,Loc}} = 2f_{\text{NL}}^{\text{Iso,Loc}} \int r^2 dr [\beta_{Xl_1}^{\text{Iso}}(r)\beta_{Yl_2}^{\text{Iso}}(r)\alpha_{Zl_3}^{\text{Iso}}(r) + \beta_{Xl_1}^{\text{Iso}}(r)\alpha_{Yl_2}^{\text{Iso}}(r)\beta_{Zl_3}^{\text{Iso}}(r) + \alpha_{Xl_1}^{\text{Iso}}(r)\beta_{Yl_2}^{\text{Iso}}(r)\beta_{Zl_3}^{\text{Iso}}(r)], \quad (15)$$

where  $\alpha_{Xl}^{\text{Iso}}$  and  $\beta_{Xl}^{\text{Iso}}$  are defined with the isocurvature radiation transfer function  $g_{Xl}^{\text{Iso}}$  as

$$\alpha_{Xl}^{\text{Iso}}(r) \equiv \frac{2}{\pi} \int k^2 dk g_{Xl}^{\text{Iso}}(k) j_l(kr), \quad (16)$$

$$\beta_{Xl}^{\text{Iso}}(r) \equiv \frac{2}{\pi} \int k^2 dk P_\eta(k) g_{Xl}^{\text{Iso}}(k) j_l(kr). \quad (17)$$

### 2.3.2 Quadratic-type isocurvature component

When the linear Gaussian term is negligible compared with the quadratic term, the isocurvature perturbation has a  $\chi^2$  from (e.g. Linde & Mukhanov 1997):

$$\mathcal{S}(\text{Quad}) = \sigma^2 - \langle \sigma^2 \rangle, \quad (18)$$

where  $\sigma$  obeys Gaussian statistics. This form has been studied in the context of axion (Kawasaki et al. 2008) and curvaton scenarios (Langlois, Vernizzi & Wands 2008). The bispectra are calculated as (Komatsu 2002)

$$B_{XYZ,l_1l_2l_3}^{\text{Iso,Quad}}(k_1, k_2, k_3) = \frac{8}{3} \int_{L_{\text{box}}^{-1}} \frac{d^3 \mathbf{p}}{(2\pi)^3} P_\sigma(\mathbf{p}) \times [P_\sigma(|\mathbf{k}_1 + \mathbf{p}|)P_\sigma(|\mathbf{k}_2 - \mathbf{p}|) + P_\sigma(|\mathbf{k}_2 + \mathbf{p}|)P_\sigma(|\mathbf{k}_3 - \mathbf{p}|) + P_\sigma(|\mathbf{k}_3 + \mathbf{p}|)P_\sigma(|\mathbf{k}_1 - \mathbf{p}|)], \quad (19)$$

where a finite box-size  $L_{\text{box}}$  gives an infrared cut-off. To avoid assumptions at scales far beyond the present horizon  $H_0^{-1}$ , we set  $L_{\text{box}} = 30$  Gpc. Equation (19) is approximately given by Hikage et al. (2009) as

$$b_{XYZ,l_1l_2l_3}^{\text{Iso,Quad}} = 2 \int r^2 dr [\beta_{Xl_1}^{\text{Iso,Quad}}(r)\beta_{Yl_2}^{\text{Iso}}(r)\alpha_{Zl_3}^{\text{Iso}}(r) + \beta_{Xl_1}^{\text{Iso}}(r)\alpha_{Yl_2}^{\text{Iso}}(r)\beta_{Zl_3}^{\text{Iso,Quad}}(r) + \alpha_{Xl_1}^{\text{Iso}}(r)\beta_{Yl_2}^{\text{Iso,Quad}}(r)\beta_{Zl_3}^{\text{Iso}}(r)], \quad (20)$$

where

$$\beta_{Xl}^{\text{Iso,Quad}}(r) \equiv \frac{2}{\pi} \int_{L_{\text{box}}^{-1}} k^2 dk P_{\mathcal{S}(\text{Quad})}(k) g_{Xl}^{\text{Iso}}(k) j_l(kr), \quad (21)$$

$$\beta_{Xl}^{\text{Iso}}(r) \equiv \frac{2}{\pi} \int_{L_{\text{box}}^{-1}} k^2 dk P_\sigma(k) g_{Xl}^{\text{Iso}}(k) j_l(kr). \quad (22)$$

The NG is proportional to  $f_{\mathcal{S}(\text{Quad})}^{3/2}$  where  $f_{\mathcal{S}(\text{Quad})}$  is the fractional isocurvature perturbation in the quadratic form:

$$f_{\mathcal{S}(\text{Quad})} = \frac{P_{\mathcal{S}(\text{Quad})}}{P_{\mathcal{S}}} f_{\mathcal{S}}. \quad (23)$$

### 2.4 Point source component

Unmasked point sources (e.g. radio galaxies) generate an additional NG in observed CMB maps. Assuming them to be Poisson distribution,  $b_{XYZ,l_1l_2l_3}^{\text{PS}}$  is a constant.

## 3 FISHER INFORMATION ANALYSIS FOR SKEW SPECTRUM

We make Fisher information analysis of the different NG components introduced in the previous section to estimate the error expected from *WMAP*, *Planck* and noiseless ideal observations.

The Fisher matrix for the CMB bispectrum in the weakly non-Gaussian, all-sky limit is written as (Babich & Zaldarriaga 2004; Yadav, Komatsu & Wandelt 2007)

$$F^{ij} = \sum_l F_l^{ij}, \quad (24)$$

$$F_l^{ij} = \sum_{2 \leq l_1 \leq l_2 \leq l} I_{l_1l_2l}^2 \sum_{XYZ} \sum_{PQR} \times b_{XYZ,l_1l_2l}^i (\text{Cov}^{-1})_{l_1l_2l}^{XYZ|PQR} b_{PQR,l_1l_2l}^j, \quad (25)$$

where  $i$  and  $j$  denote each NG component and the factor  $I_{l_1l_2l_3}$  is defined as

$$I_{l_1l_2l_3} \equiv \sqrt{\frac{(2l_1+1)(2l_2+1)(2l_3+1)}{4\pi}} \begin{pmatrix} l_1 & l_2 & l_3 \\ 0 & 0 & 0 \end{pmatrix}. \quad (26)$$

The sums over  $XYZ$  and  $PQR$  are just  $TTT$  when using CMB temperature maps only ( $T$  only), but are eight combinations ( $TTT$ ,  $TTE$ ,  $TET$ ,  $ETT$ ,  $TEE$ ,  $ETE$ ,  $EET$ ,  $EEE$ ) when both CMB temperature and  $E$  polarization maps are used ( $T&E$ ). The Fisher matrix at each  $l$ ,  $F_l^{ij}$ , is associated with the skew spectrum estimator for the  $i$ th NG component,  $S_l^i$ , defined as (Munshi & Heavens 2010)

$$S_l^i = \frac{1}{2l+1} \sum_{2 \leq l_1 \leq l_2 \leq l} I_{l_1l_2l}^2 \sum_{XYZ} \sum_{PQR} \times b_{XYZ,l_1l_2l}^i (\text{Cov}^{-1})_{l_1l_2l}^{XYZ|PQR} b_{PQR,l_1l_2l}^{\text{obs}}, \quad (27)$$

where  $b_{l_1l_2l}^{\text{obs}}$  denotes the observed bispectrum. The relation to the single skewness estimator  $S_{\text{prim}}^i$  (Komatsu et al. 2005) is

$$S_{\text{prim}}^i = \sum_l (2l+1) S_l^i. \quad (28)$$

When NG is small, the covariance matrix is approximately given by

$$\text{Cov}_{l_1l_2l_3}^{XYZ|PQR} \simeq \Delta_{l_1l_2l_3} C_{l_1}^{XP} C_{l_2}^{YQ} C_{l_3}^{ZR}, \quad (29)$$

where  $\Delta_{l_1l_2l_3}$  is 6 ( $l_1 = l_2 = l_3$ ), 2 ( $l_1 = l_2, l_2 = l_3$  or  $l_1 = l_3$ ) and 1 ( $l_1 \neq l_2 \neq l_3$ ) and  $C_l^{XY}$  represents the CMB power spectrum from purely adiabatic perturbations including observational noise  $N_l^{XY}$ :

$$C_l^{XY} = \frac{2}{\pi} \int k^2 dk P_\phi(k) g_{Xl}^{\text{Adi}}(k) g_{Yl}^{\text{Adi}}(k) + N_l^{XY}. \quad (30)$$

We consider three different noise/beam functions: an ideal case without noise/beam ('Ideal'); *WMAP* 5-year  $V+W$ -band co-added map ('*WMAP5*'); *Planck*'s expectations after two full sky surveys

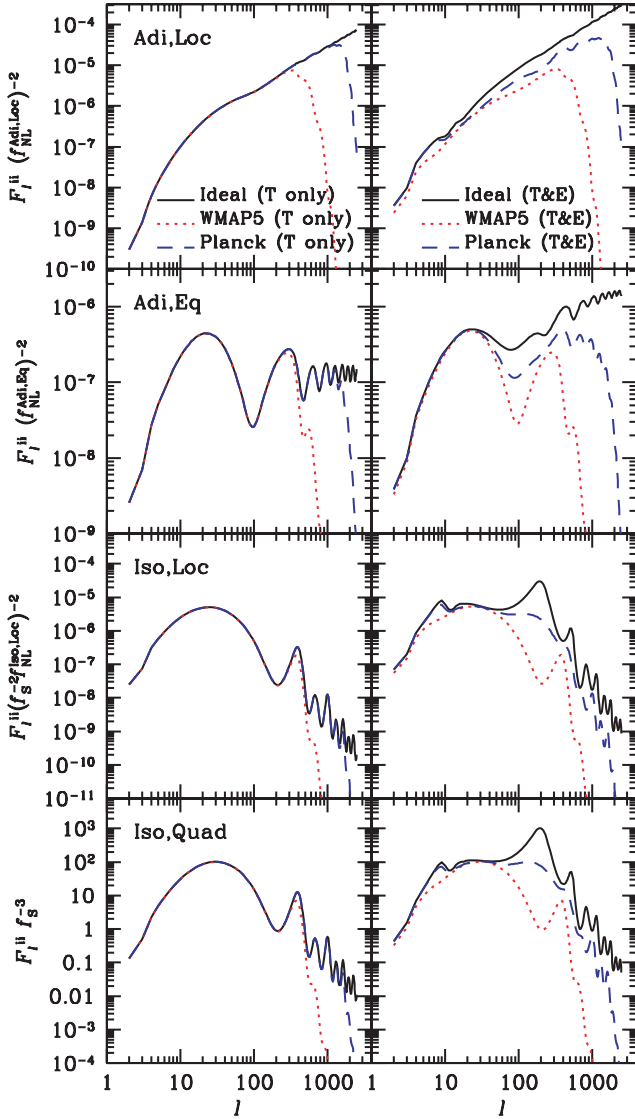


**Figure 1.** Diagonal components of the Fisher matrix  $F_{ii}^{ii}$  (equation 25). From top to bottom, the local-type adiabatic (Adi,Loc), the equilateral-type adiabatic (Adi,Eq), the local-type isocurvature (Iso,Loc) and the quadratric-type isocurvature (Iso,Quad) components are plotted. Left-hand panels are for  $T$  map only, but right-hand panels are for  $T&E$  maps. Noise/Beam is for Ideal (solid), *WMAP5* (dotted) and *Planck* observations (dashed).

for 14 months (*Planck*) using all of nine frequency channels. Noise is assumed to be homogeneous white noise and  $N_i^{XY} = 0$  when  $X \neq Y$ . Noise/beam is co-added at each  $l$  with the inverse weight of the noise variance in each frequency band or differential assembly. *Planck*'s noise/beam information is obtained from <http://www.rssd.esa.int/Planck>. The fraction of sky  $f_{\text{sky}}$  is set to be 1 in this analysis.

Fig. 1 shows the diagonal component of the Fisher matrix  $F_{ii}^{ii}$  (equation 25). It represents the square of S/N  $[(S/N)^2]$  for  $i$ th NG component at  $l$  without correlations among different NG components. The local adiabatic component increases in proportion to  $l$  at  $l > 20$ . The equilateral one is more flat using temperature spectrum only, while it grows more rapidly including  $E$  polarization. The results can be explained as follows: the local-type adiabatic NG is sensitive to the bispectrum with squeezed-shape triangles ( $l_1 \ll l_2 \simeq l_3$ ). As the bispectrum  $b(l_1, l_2, l_3)$  is roughly proportional to  $C_{l_1} C_{l_2} + C_{l_2} C_{l_3} + C_{l_3} C_{l_1}$ , the  $(S/N)^2$  of a squeezed-shape bispectrum is  $b(l_1, l_2, l_3)^2 / C_{l_1} C_{l_2} C_{l_3} \propto (C_{l_1} C_{l_1})^2 / (C_{l_1} C_{l_1}^2) = C_{l_1}$ , which is insensitive to  $l$ . The number of squeezed triangles significantly contributing to  $(S/N)^2$  increases very slowly by  $l$ . Actually 80 per cent of  $(S/N)^2$  come from the bispectrum with  $l_1$  less than 20 for  $l = 500$ , 22 for  $l = 1000$  and 25 for  $l = 1500$ . In consequence,  $F_i$  increases with the factor  $l^2$ , which is proportional to  $l$ . The equilateral-type NG is sensitive to the equilateral-shape bispectrum, the  $(S/N)^2$  of which changes as  $b_{l_1 l_2 l_3}^2 / C_{l_1}^3 \propto C_l$ . The temperature spectrum  $C_l^{TT}$  is roughly proportional to  $l^{-2}$  at small  $l$  and more steeply decreases as  $\propto l^{-4}$  at  $l > 1000$ . The decrement is well cancelled in  $F_i$  because the number of triangles increases in proportional to  $l^2$  and the factor  $l^2 / l^4 \propto l^{-2}$ . Including the  $E$  polarization spectrum, which has different scale dependence as  $C_l^{TE} \propto l^{-1}$  and  $C_l^{EE}$  is nearly constant at  $l < 1000$ ,  $F_i$  grows more rapidly.

The isocurvature NGs are sensitive to squeezed-shape bispectra as the local-type adiabatic one, but the  $(S/N)^2$  becomes  $(b_{l_1 l_2 l_3}^{\text{Iso}})^2 / C_{l_1}^{\text{Iso}} C_{l_2}^{\text{Iso}} C_{l_3}^{\text{Iso}} \propto (C_l^{\text{Iso}} / C_l^{\text{Adi}})^2$ , which decreases as  $l^{-4}$ . Including the scale dependence of the factor  $l^2 / l^4 \propto l^{-2}$ ,  $F_i$  of isocurvature modes is proportional to  $l^{-3}$  as shown in Fig. 1. The majority of the signal of the isocurvature components in temperature maps come from the large-angular scale ( $l < 100$ ), where isocurvature perturbations produce larger CMB fluctuations than adiabatic perturbations. A phase difference in acoustic oscillations between adiabatic and isocurvature modes provides a distinct signature seen around  $l \sim 300$ , which is important particularly when polarization maps are included.

Table 1 lists the values of the diagonal components of the Fisher matrix summed over  $l$  up to 2500, at which *Planck* estimates are

**Table 1.** Diagonal components of the Fisher matrix  $F_{ii}^{ii}$  summed up to  $l = 2500$ . The different noise/beam for *WMAP5*, *Planck* and Ideal are considered.

	Adi,Loc	Adi,Eq	Iso,Loc	Iso,Quad
<i>WMAP5</i> ( $T$ only)	$2.7 \times 10^{-3} (f_{\text{NL}}^{\text{Adi,Loc}})^2$	$7.2 \times 10^{-5} (f_{\text{NL}}^{\text{Adi,Eq}})^2$	$2.9 \times 10^{-4} [f_{\text{S(Lin)}}^2 f_{\text{NL}}^{\text{Iso,Loc}}]^2$	$6.8 \times 10^3 f_{\text{S(Quad)}}^3$
<i>Planck</i> ( $T$ only)	$3.7 \times 10^{-2} (f_{\text{NL}}^{\text{Adi,Loc}})^2$	$2.3 \times 10^{-4} (f_{\text{NL}}^{\text{Adi,Eq}})^2$	$3.1 \times 10^{-4} [f_{\text{S(Lin)}}^2 f_{\text{NL}}^{\text{Iso,Loc}}]^2$	$7.6 \times 10^3 f_{\text{S(Quad)}}^3$
Ideal ( $T$ only)	$9.0 \times 10^{-2} (f_{\text{NL}}^{\text{Adi,Loc}})^2$	$3.4 \times 10^{-4} (f_{\text{NL}}^{\text{Adi,Eq}})^2$	$3.1 \times 10^{-4} [f_{\text{S(Lin)}}^2 f_{\text{NL}}^{\text{Iso,Loc}}]^2$	$7.7 \times 10^3 f_{\text{S(Quad)}}^3$
<i>WMAP5</i> ( $T&E$ )	$3.0 \times 10^{-3} (f_{\text{NL}}^{\text{Adi,Loc}})^2$	$7.5 \times 10^{-5} (f_{\text{NL}}^{\text{Adi,Eq}})^2$	$3.1 \times 10^{-4} [f_{\text{S(Lin)}}^2 f_{\text{NL}}^{\text{Iso,Loc}}]^2$	$7.2 \times 10^3 f_{\text{S(Quad)}}^3$
<i>Planck</i> ( $T&E$ )	$5.8 \times 10^{-2} (f_{\text{NL}}^{\text{Adi,Loc}})^2$	$4.8 \times 10^{-4} (f_{\text{NL}}^{\text{Adi,Eq}})^2$	$8.9 \times 10^{-4} [f_{\text{S(Lin)}}^2 f_{\text{NL}}^{\text{Iso,Loc}}]^2$	$2.6 \times 10^4 f_{\text{S(Quad)}}^3$
Ideal ( $T&E$ )	$3.6 \times 10^{-1} (f_{\text{NL}}^{\text{Adi,Loc}})^2$	$2.9 \times 10^{-3} (f_{\text{NL}}^{\text{Adi,Eq}})^2$	$3.9 \times 10^{-3} [f_{\text{S(Lin)}}^2 f_{\text{NL}}^{\text{Iso,Loc}}]^2$	$1.3 \times 10^5 f_{\text{S(Quad)}}^3$

enough saturated. The result of the adiabatic local NG from temperature only maps is consistent with the previous work by Komatsu & Spergel (2001), which has  $3.4 \times 10^{-3} f_{\text{NL}}^2$  for *WMAP* and  $3.8 \times 10^{-2} f_{\text{NL}}^2$  for *Planck* (the details depend on the assumed cosmology and beam/noise properties). When the information of *E* polarization is included, the total Fisher matrix  $F = (S/N)^2$  becomes four

times larger in the ideal case. This is consistent with the result of Babich & Zaldarriaga (2004) showing that S/N is twice better with *E* polarization included.

Fig. 2 shows the cross-correlation coefficient  $r_l$  defined as  $r_l \equiv F_l^{ij} / (F_l^{ii} F_l^{jj})^{1/2}$ . The local-type adiabatic and isocurvature components are strongly correlated, but the phase difference of acoustic

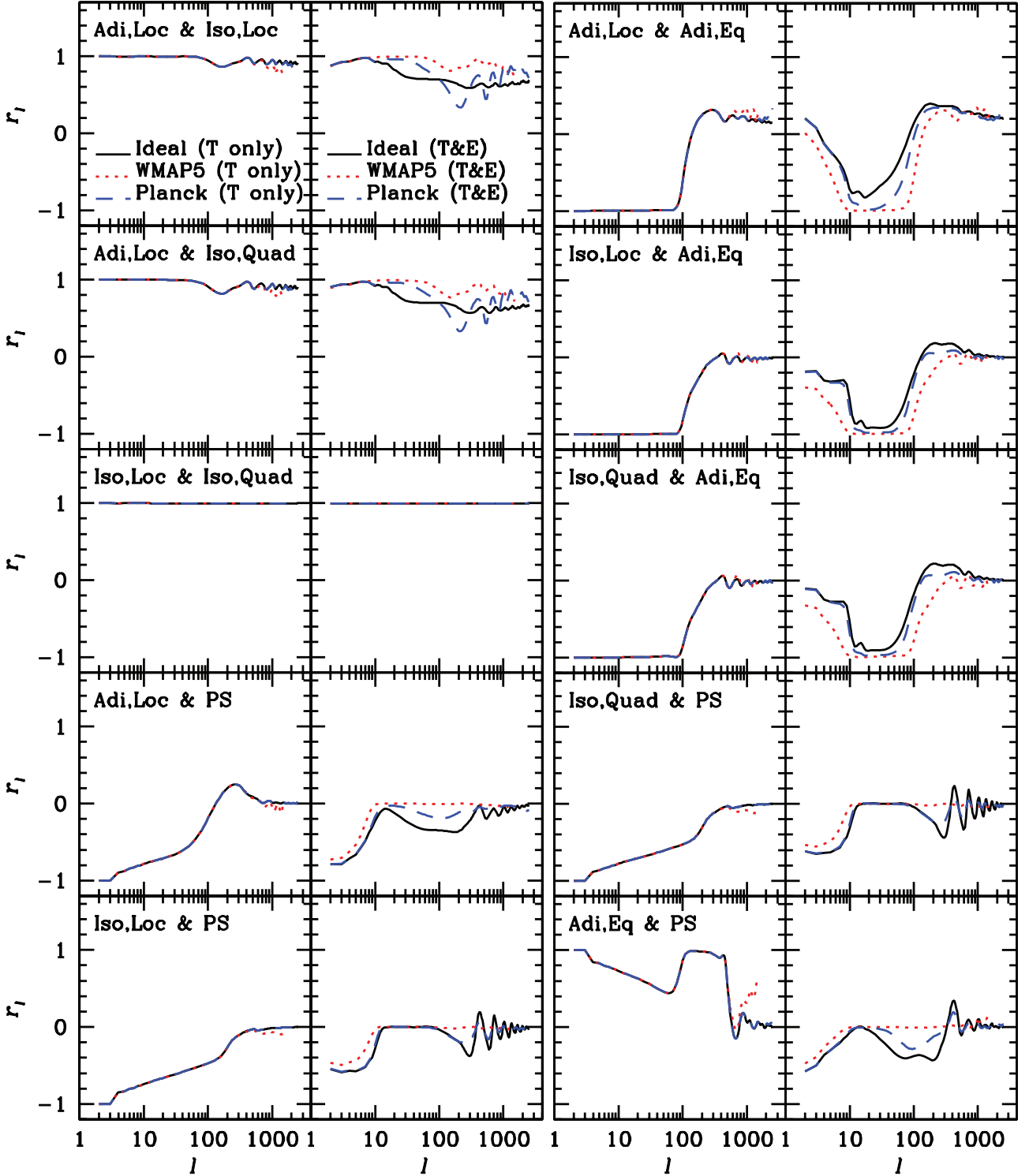


**Figure 2.** Cross-correlation coefficients  $r_l^{ij} \equiv F_l^{ij} / (F_l^{ii} F_l^{jj})^{1/2}$  where  $i$  and  $j$  denote the local-type adiabatic (Adi,Loc), the local-type isocurvature (Iso,Loc), the equilateral-type adiabatic (Adi,Eq), the quadratic-type isocurvature (Iso,Quad) and the point source (PS) components. The left of each panel is temperature *T* only; the right is *T*&*E*, including *E* polarization. Noise/Beam is for Ideal (solid), *WMAP*5 (dotted) and *Planck* observations (dashed).

oscillations weakens the correlation, as seen especially around  $l \sim 200$ . The correlation between the local-type and the equilateral-type components becomes weak at  $l > 100$ . The two isocurvature components with scale-invariant spectra are almost completely correlated at all scales. This is explained as follows: if all of the spectra of  $\eta$  (equation 12),  $\sigma$  (equation 18) and  $\mathcal{S}(\text{Quad})$  are scale-invariant, their isocurvature bispectra (equations 15 and 20) have same configuration dependence and thereby their cross-correlation coefficient is unity. When  $\sigma$  is assumed to be scale-invariant spectrum, the power spectrum of  $\mathcal{S}(\text{Quad})$  has an additional scale-dependent factor  $\log(kL_{\text{box}})$  (see equation 38 in Hikage et al. 2009). The effect is, however, very small and  $r$  is still close to unity.

The correlation with the point source component is very weak for  $l > 100$ .

Fig. 3 shows  $1\sigma$  error contours (Cramér–Rao bound) for a pair of NG parameters for *WMAP5* ( $T$  only), *Planck* ( $T$  only) and *Planck* ( $T&E$ ). The errors expected from *WMAP5* ( $T&E$ ) is almost same as those from *WMAP5* ( $T$  only). The rest of NG parameters other than the two plotted are fixed to be zero. The local-type adiabatic

and isocurvature components are correlated with the correlation coefficient  $r = 0.43$  for *WMAP5*,  $r = 0.23$  for *Planck*  $T$  only,  $r = 0.20$  for *Planck*  $T&E$  when  $l$  is summed up to 2500. We see that the local-type and the quadratic-type scale-invariant isocurvature components are difficult to be differentiated even using *Planck* data. The local-type and the equilateral-type adiabatic components are weakly correlated ( $r = 0.12$  for *WMAP5*,  $r = 0.17$  for *Planck*  $T$  only,  $r = 0.22$  for *Planck*  $T&E$ ), which is consistent with the previous work (Babich et al. 2004). The point source component is almost uncorrelated with the other primordial components ( $r < 0.08$  for *WMAP5* and  $r < 0.03$  for *Planck*), which is consistent with the previous work (Komatsu & Spergel 2001). Table 2 lists the errors of the NG parameters without and with correlations among all of other parameters except for the quadratic-type isocurvature component. Polarization maps are found to be very important to constrain the isocurvature NG as well as adiabatic NG. The increase of the errors due to the correlations mainly between adiabatic and isocurvature modes is 20–30 per cent for *WMAP5*, but less than 5 per cent for *Planck* observations.

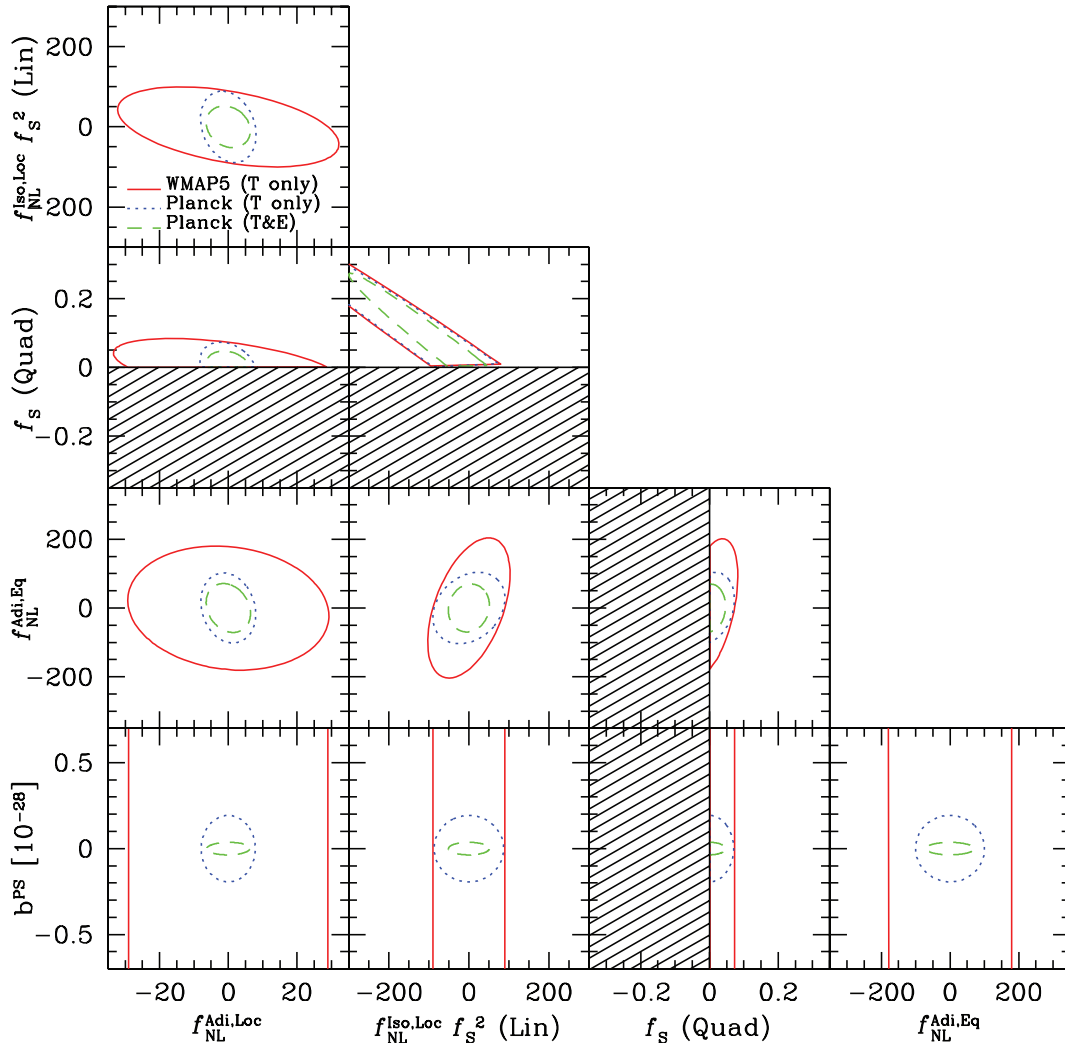


**Figure 3.**  $1\sigma$  error contours of a pair of NG parameters expected from *WMAP5*  $T$  only (solid circles), *Planck*  $T$  only (dotted circles) and *Planck*  $T&E$  (dashed circles). The isocurvature fraction is a non-negative value and thereby the area with negative values of  $f_{\mathcal{S}(\text{Quad})}$  is shaded. The rest of NG parameters other than the two plotted are fixed to be zero.

**Table 2.**  $1\sigma$  errors of each NG parameter from the joint analysis of all of the NG components except for the quadratic-type isocurvature components. The values without parentheses denote the limits with other parameters fixed, but those with parentheses denote the limits including the correlations such that the other parameters are marginalized.

	<i>WMAP5</i>		<i>Planck</i>	
	<i>T</i> only	<i>T</i> only	<i>T</i> only	<i>T&amp;E</i>
$\Delta f_{\text{NL}}^{\text{Adi,Loc}}$	19 (23)	5.2 (5.5)	4.1 (4.3)	
$\Delta f_{\text{S(Lin)}}^2 f_{\text{NL}}^{\text{Iso,Loc}}$	59 (82)	57 (62)	34 (35)	
$\Delta f_{\text{NL}}^{\text{Adi,Eq}}$	117 (149)	66 (71)	46 (48)	
$\Delta b^{\text{PS}} [10^{-28}]$	438 (441)	0.13 (0.13)	0.024 (0.024)	

#### 4 SUMMARY

We have presented a detailed analysis of the possibility of extracting information about NG from various inflationary models. We consider four different types of primordial NG models: local-type adiabatic, equilateral-type adiabatic, local-type isocurvature and quadratic-type isocurvature models together with point source contamination. The adiabatic and the isocurvature modes are correlated, but the difference in the phase of the corresponding acoustic oscillations breaks the degeneracy. The local-type and quadratic-type scale-invariant isocurvature components are difficult to separate even using *Planck* data. The correlation between the local-type and the equilateral-type adiabatic modes is weak. The point source (white noise) contamination does not pose a threat as it is uncorrelated with any of the  $f_{\text{NL}}$  parameters, although a high-resolution experiment will be more suited to get rid of such contamination. Our results are based on noise models from *WMAP* and *Planck* and we compare them to ideal noise-free and all-sky reference observations. The increase of the error for the non-Gaussian parameters due to the correlations is 20–30 per cent for *WMAP5* and 5 per cent for *Planck*.

Secondary anisotropies other than point sources can contaminate the estimation of primordial NG. The cross-contamination of various inflationary contributions against secondaries such as Sunyaev–Zeldovich effect or integrated Sachs–Wolfe effect which are potentially observable with *Planck* data will be present elsewhere.

#### ACKNOWLEDGMENTS

CH acknowledges support from a Japan Society for the Promotion of Science (JSPS) fellowship. DM acknowledges financial support from an STFC rolling grant at the University of Edinburgh.

#### REFERENCES

Acquaviva V., Bartolo N., Matarrese S., Riotto A., 2003, *Nuclear Phys. B*, 667, 119  
 Alishahiha M., Silverstein E., Tong T., 2004, *Phys. Rev. D*, 70, 123505  
 Arkani-Hamed N., Creminelli P., Mukohyama S., Zaldarriaga M., 2004, *J. Cosmology Astropart. Phys.*, 4, 1  
 Babich D., Zaldarriaga M., 2004, *Phys. Rev. D*, 70, 083005  
 Babich D., Creminelli P., Zaldarriaga M., 2004, *J. Cosmology Astropart. Phys.*, 8, 9  
 Bartolo N., Komatsu E., Matarrese S., Riotto A., 2004a, *Phys. Rep.*, 402, 103

Bartolo N., Matarrese S., Riotto A., 2004b, *Phys. Rev. D*, 69, 043503  
 Bartolo N., Matarrese S., Riotto A., 2006, *J. Cosmol. Astropart. Phys.*, 6, 24  
 Bean R., Dunkley J., Pierpaoli E., 2006, *Phys. Rev. D*, 74, 063503  
 Beltran M., 2008, *Phys. Rev. D*, 78, 023530  
 Boubekeur L., Creminelli P., 2006, *Phys. Rev. D*, 73, 103516  
 Boubekeur L., Lyth D. H., 2006, *Phys. Rev. D*, 73, 021301  
 Buchbinder E. I., Khoury J., Ovrut B. A., 2007, *J. High Energy Phys.*, 11, 76  
 Cabella P., Hansen F. K., Liguori M., Marinucci D., Matarrese S., Moscardini L., Vittorio N., 2006, *MNRAS*, 369, 819  
 Chen X., Easther R., Lim E. A., 2007, *J. Cosmol. Astropart. Phys.*, 6, 23  
 Creminelli P., Senatore L., 2007, *J. Cosmol. Astropart. Phys.*, 11, 10  
 Creminelli P., Nicolis A., Senatore L., Tegmark M., Zaldarriaga M., 2006, *J. Cosmol. Astropart. Phys.*, 5, 4  
 Creminelli P., Senatore L., Zaldarriaga M., 2007, *J. Cosmol. Astropart. Phys.*, 3, 19  
 Dunkley J. et al., 2009, *ApJS*, 180, 306  
 Dvali G., Gruzinov A., Zaldarriaga M., 2004, *Phys. Rev. D*, 69, 083505  
 Falk T., Madden R., Olive K. A., Srednicki M., 1993, *Phys. Lett. B*, 318, 354  
 Gangui A., Lucchin F., Matarrese S., Mollerach S., 1994, *ApJ*, 430, 447  
 Gupta S., Berera A., Heavens A. F., Matarrese S., 2002, *Phys. Rev. D*, 66, 043510  
 Heavens A. F., 1998, *MNRAS*, 299, 805  
 Hikage C., Koyama K., Matsubara T., Takahashi T., Yamaguchi M., 2009, *MNRAS*, 398, 2188  
 Kawasaki M., Nakayama K., Sekiguchi T., Suyama T., Takahashi F., 2008, *J. Cosmol. Astropart. Phys.*, 11, 19  
 Kawasaki M., Nakayama K., Takahashi F., 2009, *J. Cosmol. Astropart. Phys.*, 1, 2  
 Komatsu E., 2002, preprint (astro-ph/0206039)  
 Komatsu E., Spergel D. N., 2001, *Phys. Rev. D*, 63, 3002  
 Komatsu E., Spergel D. N., Wandelt B. D., 2005, *ApJ*, 634, 14  
 Komatsu E. et al., 2009, *ApJS*, 180, 330  
 Koyama K., Mizuno S., Vernizzi F., Wands D., 2007, *J. Cosmol. Astropart. Phys.*, 11, 24  
 Langlois D., Vernizzi F., Wands D., 2008, *J. Cosmol. Astropart. Phys.*, 12, 4  
 Liguori M., Yadav A., Hansen F. K., Komatsu E., Matarrese S., Wandelt B., 2007, *Phys. Rev. D*, 76, 105016  
 Linde A. D., Mukhanov V., 1997, *Phys. Rev. D*, 56, R535  
 Lyth D. H., Ungarelli C., Wands D., 2003, *Phys. Rev. D*, 67, 023503  
 Maldacena J. M., 2003, *J. High Energy Phys.*, 5, 13  
 Medeiros J., Contaldi C. R., 2006, *MNRAS*, 367, 39  
 Moroi T., Takahashi T., 2009, *Phys. Lett. B*, 671, 339  
 Moss I., Xiong C., 2007, *J. Cosmol. Astropart. Phys.*, 4, 7  
 Munshi D., Heavens A., 2010, *MNRAS*, 401, 2406  
 Peebles P. J. E., 1999, *ApJ*, 510, 531  
 Salopek D. S., Bond J. R., 1990, *Phys. Rev. D*, 42, 3936  
 Seery D., Lidsey J. D., 2005, *J. Cosmol. Astropart. Phys.*, 6, 3  
 Seljak U., Zaldarriaga M., 1996, *ApJ*, 469, 437  
 Smith K. M., Zaldarriaga M., 2006, preprint (astro-ph/0612571)  
 Smith K. M., Senatore L., Zaldarriaga M., 2009, *J. Cosmol. Astropart. Phys.*, 9, 6  
 Suyama T., Takahashi F., 2008, *J. Cosmol. Astropart. Phys.*, 9, 7  
 Verde L., Wang L., Heavens A. F., Kamionkowski M., 2000, *MNRAS*, 313, 141  
 Wang L., Kamionkowski M., 2000, *Phys. Rev. D*, 61, 63504  
 Yadav A. P. S., Wandelt B. D., 2008, *Phys. Rev. Lett.*, 100, 181301  
 Yadav A. P. S., Komatsu E., Wandelt B. D., 2007, *ApJ*, 664, 680

This paper has been typeset from a  $\text{\TeX}/\text{\LaTeX}$  file prepared by the author.